

## HIGH-RESOLUTION STUDIES OF GAS AND DUST AROUND YOUNG INTERMEDIATE-MASS STARS. II. OBSERVATIONS OF AN ADDITIONAL SAMPLE OF HERBIG Ae SYSTEMS

VINCENT MANNINGS

Jet Propulsion Laboratory, California Institute of Technology, MS 169-327, 4800 Oak Grove Drive, Pasadena, CA 91109

AND

ANNELA I. SARGENT

Division of Physics, Mathematics and Astronomy, California Institute of Technology, MS 105-24, Pasadena, CA 91125

Received 1999 March 30; accepted 1999 July 16

### ABSTRACT

In an earlier paper (Mannings & Sargent; Paper I), we presented evidence for disks of gas and dust associated with seven Herbig Ae stars, based on high-resolution interferometric millimeter-wave observations of continuum and molecular line emission. These systems are simultaneously high-mass analogs of the approximately solar-mass T Tauri stars and the evolutionary precursors of the prototypical main-sequence debris-disk sources  $\beta$  Pic,  $\alpha$  Lyr, and  $\alpha$  PsA. Here we extend the original survey to include four additional Herbig Ae systems. We have also imaged two of the sources from Paper I at higher resolution. The new data are presented and analyzed, and are combined with the results from the earlier sample in order to address the properties of this class of circumstellar disk. Derived disk masses are indistinguishable from the masses of T Tauri disks. Although the combined sample is small, it seems likely that disk masses are essentially uncorrelated with stellar mass for pre-main-sequence stars of spectral type A0 and later.

*Subject headings:* accretion, accretion disks — circumstellar matter — stars: pre-main-sequence

### 1. INTRODUCTION

Herbig Ae stars are young emission-line stars in the pre-main-sequence phase of evolution, with masses of around 2–5  $M_{\odot}$  (Herbig 1960, 1994). Their properties are described comprehensively in excellent reviews by Pérez & Grady (1997) and Waters & Waelkens (1998). In common with T Tauri stars (TTs) of later spectral type, they are often found in association with nebulosity, exhibit strong metallic and Balmer spectral lines, have energetic stellar winds, often display rapid photometric and spectroscopic variability, and show continuum excesses above photospheric levels. For the TTs, continuum excesses from IR to millimeter wavelengths are due to thermal emission from grains in circumstellar disks (see reviews by Beckwith & Sargent 1993a; Strom, Edwards, & Skrutskie 1993; Sargent 1996). In contrast, excesses observed toward Herbig Ae stars have been variously interpreted (see the review by Natta, Grinin, & Mannings 2000). Explanations include emission from grains distributed in compact circumstellar disks with radii of several hundred AU (Hillenbrand et al. 1992; Natta et al. 1997), grain emission from extended envelopes with radii  $\sim 10^4$  AU (Berrilli et al. 1992; Di Francesco et al. 1994; Miroshnichenko, Ivezić, & Elitzur 1997; Pezzuto, Strafella, & Lorenzetti 1997), and emission from combinations of small disks and large envelopes (Natta et al. 1992; 1993). The fact that each of these geometries is equally successful in fitting the continuum spectral energy distributions of Herbig Ae stars is due principally to low angular resolution, typically  $10''$ – $30''$  at far-IR and millimeter wavelengths.

In an earlier paper (Mannings & Sargent 1997; hereafter Paper I), we described the first results from our interferometric millimeter-wave continuum and line survey of Herbig Ae stars at resolutions of  $2''$ – $5''$ . Compact continuum emission, centered on the stars, was detected in all seven of the sources observed. Most of the dust regions were not spatially resolved, with typical upper limits to radii of about 300 AU. Estimated masses of circumstellar dust and gas

were in the range 0.005–0.034  $M_{\odot}$ . Molecular line emission was detected from compact regions centered on four of the stars. In the two spatially resolved cases, HD 163296 and AB Aur, ordered gas velocity gradients were observed, which is consistent with Keplerian rotation in a disk. For these objects, aspherical gas morphologies, negligible optical extinctions, double-peaked millimeter-wave line spectra, and narrow line widths also argue for orbiting material in disklike configurations. By analogy, we argued that the nebular environments of the entire sample probably include substantial disk components. This was subsequently confirmed for the star MWC 480 using higher resolution measurements and kinematic modeling (Mannings, Koerner, & Sargent 1997).

The measured masses and radii for Herbig Ae disks appear remarkably similar to those for the disks surrounding the TTs (Paper I). The latter disks have masses of between 0.001 and 0.1  $M_{\odot}$  and outer radii typically in the range 100–500 AU (e.g., Beckwith et al. 1990, hereafter BSCG; André & Montmerle 1994; Koerner & Sargent 1995; Osterloh & Beckwith 1995; Dutrey et al. 1996, 1998). We suggested in Paper I that, for stars of spectral type A0 and later, the bulk properties of circumstellar disks during the early stages of pre-main-sequence (hereafter pre-MS) stellar evolution may be independent of stellar mass. Here we test this conclusion using new observations of four additional Herbig Ae stars, as well as higher frequency observations of two targets from Paper I. In §§ 2 and 3 we describe the selection of sources and give details of the observations. The results are presented and analyzed in § 4 and discussed in § 5.

### 2. THE SAMPLE

For the reasons given in Paper I, we continue to concentrate on stars of spectral type Ae rather than Be. Identification as pre-MS objects is more secure for Herbig Ae stars than it is for Herbig Be stars (cf. Calvet et al. 1994), and the

cataloged Herbig Ae sources are, on average, much nearer than their Herbig Be counterparts, enabling better spatial resolution. Perhaps most intriguing, Herbig Ae stars occupy the same range of spectral types as the main-sequence debris-disk stars  $\alpha$  Lyr (A0 V),  $\alpha$  PsA (A3 V), and  $\beta$  Pic (A5 V) (cf. Backman & Paresce 1993; Lagrange, Backman, & Artymowicz 2000), suggesting that studies of very young Ae sources will help probe the origins of these debris disks. As before, we have biased our sample toward compact, non-embedded sources by selecting only targets that exhibit mid- and far-IR continuum spectral energy distributions (SEDs  $\equiv \log vF_\nu$  vs.  $\log \nu$ ) that decline with increasing wavelength, similar to those of optically visible TTs surrounded by inclined circumstellar disks (Adams, Lada, & Shu 1987; 1988).

The Ae targets are listed in Table 1, together with coordinates, spectral types, distances, single-dish 1.3 mm flux densities, and submillimeter spectral indices. We also tabulate total  $V$ -band extinctions,  $A_V$ . While most of these are taken from the literature, we estimate the  $A_V$  toward LkH $\alpha$  259 using the cataloged spectral type, observed  $B$  and  $V$  magnitudes, the Schmidt-Kaler (1982) table of standard values of  $(B-V)$  colors, and an assumed ratio of total to selective absorption,  $R = 3.1$ . We also tabulate photospheric temperatures (Cohen & Kuhi 1979) together with our estimates of stellar radii, luminosities, masses, and ages (see § 5). As in Paper I, we have given preference to the nearer of the cataloged Herbig Ae stars (Thé, de Winter, & Pérez 1994) and to sources with declinations greater than  $-25^\circ$  for which single-dish millimeter-wave continuum measurements are available (Osterloh & Beckwith 1995; Sylvester et al. 1996; Mannings et al. 2000, in preparation) We have already detected MWC 758 and CQ Tau in 2.7 mm continuum emission, and unresolved  $^{13}\text{CO}$  ( $1 \rightarrow 0$ ) emission was found in association with MWC 758 (Paper I). Observations of both objects in 1.3 mm continuum and CO ( $2 \rightarrow 1$ ) line emission are reported here.

### 3. OBSERVATIONS

All measurements were made between 1996 January and 1998 January using the Owens Valley Radio Observatory (OVRO) millimeter-wave array at Big Pine, California. The array comprises six 10.4 m diameter telescopes. Com-

binations of up to three array configurations were used, with antenna spacings ranging from 15 to 200 m east-west and from 15 to 220 m north-south. The sizes of the naturally weighted synthesized beams were  $4''\text{--}5''$  (FWHM) at  $\lambda \approx 3$  mm and  $2''$  (FWHM) at  $\lambda \approx 1$  mm. Cryogenically cooled superconductor-insulator-superconductor (SIS) receivers on each telescope produced average single sideband system temperatures of 1000 and 1550 K at the frequencies of the CO ( $1 \rightarrow 0$ ) and CO ( $2 \rightarrow 1$ ) lines, respectively. For the CO ( $1 \rightarrow 0$ ) observations of MWC 614, HD 34282, MacC H12, and LkH $\alpha$  259, the digital correlator was configured to provide two bands of Hanning-smoothed channels,  $64 \times 0.5$  MHz and  $64 \times 0.125$  MHz, with velocity resolutions of 1.30 and 0.33 km s $^{-1}$ , respectively. High-resolution CO ( $2 \rightarrow 1$ ) measurements of MWC 758 and CQ Tau used bands of  $64 \times 0.125$  MHz and  $64 \times 0.5$  MHz, with corresponding velocity resolutions of 0.16 and 0.65 km s $^{-1}$ . Where there was no prior knowledge of systemic velocities, we centered spectrometer bands at  $v_{\text{LSR}} = 0$ . At all frequencies, simultaneous continuum measurements were made using an analog correlator of bandwidth 1 GHz.

Calibration of visibility phases and amplitudes was achieved with observations of quasars, typically at intervals of 20 minutes. The quasar 0528+134 was used for phase and amplitude calibration of MWC 758 and CQ Tau; 0133+476 and 0224+671 were used for both MacC H12 and LkH $\alpha$  259; 1749+096 and 2023+336 were used for MWC 614; and 0420-014 and 0607-157 were used for HD 34282. Measurements of 3C 273, 3C 345, and 3C 454.3 were made to calibrate the spectrometer passbands, and observations of Uranus and Neptune provided an absolute flux density scale. Calibration was carried out using the in-house software package, MMA (Scoville et al. 1993). Continuum and spectral line maps were generated and CLEANed using the NRAO Astronomical Image Processing System (AIPS) package. Uncertainties in fluxes and source positions are estimated to be about 20% and 0'.5, respectively. The average 1  $\sigma$  rms noise levels on the continuum maps are 2.1 and 7.3 mJy beam $^{-1}$  at  $\lambda = 2.6$  and 1.3 mm, respectively. For the spectral line channels, the average 1  $\sigma$  rms is 0.103 Jy beam $^{-1}$  ( $\Delta v = 0.65$  km s $^{-1}$ ) at CO ( $2 \rightarrow 1$ ), and 0.124 Jy beam $^{-1}$  ( $\Delta v = 1.3$  km s $^{-1}$ ) at CO ( $1 \rightarrow 0$ ).

TABLE 1  
SOURCE PARAMETERS

Star	R.A. (1950)	Decl. (1950)	Spectral Type <sup>a</sup>	$d$ (pc)	$F_{1.3 \text{ mm}}$ (mJy)	$\alpha_{\text{submm}}^b$	$A_V$	$T_{\text{eff}}^c$ (K)	$R_*^c$ ( $R_\odot$ )	$L_*^c$ ( $L_\odot$ )	$M_*^c$ ( $M_\odot$ )	Age <sup>e</sup> (Myr)
MWC 614	19 <sup>d</sup> 08 55.42	+15 42 15.1	B9/A0/IV/Ve	240 $^{+70}_{-40}$ <sup>e</sup>	...	...	1.27 <sup>e</sup>	10220	4.7	221.9	4	0.3
HD 34282	05 <sup>d</sup> 13 38.09	-09 51 51.6	A0 Ve+sh	160 $^{+60}_{-40}$ <sup>e</sup>	183 <sup>f</sup> $\pm$ 17	2.2 <sup>f</sup> $\pm$ 0.2	0.59 <sup>e</sup>	10040	0.6	4.3	...	...
MWC 758	05 <sup>d</sup> 27 22.46	+25 17 42.9	A3e	200 $^{+60}_{-40}$ <sup>e</sup>	72 <sup>b</sup> $\pm$ 13	2.80 <sup>b</sup> $\pm$ 0.21	0.22 <sup>e</sup>	8465	2.1	20.6	2	6
MacC H12	00 <sup>g</sup> 04 25.22	+65 21 56.9	A5/F:e	845 <sup>h</sup>	44 <sup>h</sup> $\pm$ 5	...	5.55 <sup>h</sup>	8270	3.0	47.1	2.5	3
CQ Tau	05 <sup>d</sup> 32 54.13	+24 43 03.9	A8 V/F2 IVe	100 $^{+25}_{-17}$ <sup>e</sup>	221 <sup>b</sup> $\pm$ 40	1.98 <sup>b</sup> $\pm$ 0.20	0.96 <sup>e</sup>	7130	1.9	8.0	1.5	10
LkH $\alpha$ 259	23 <sup>i</sup> 56 09.60	+66 09 32.0	A9 e	850	...	...	5.22 <sup>j</sup>	7320	6.5	107.3	3.5	0.3

NOTE.—Units of right ascension are hours, minutes, and seconds, and units of declination are degrees, arcminutes, and arcseconds.

<sup>a</sup> Thé et al. 1994.

<sup>b</sup> Mannings et al., in preparation.

<sup>c</sup> See § 5, this work. Values of  $T_{\text{eff}}$ ,  $R_*$ , and  $L_*$  for MWC 758 and CQ Tau are from Paper I.

<sup>d</sup> *Hipparcos* and *Tycho* Catalogues (ESA 1997).

<sup>e</sup> Van den Ancker et al. 1998.

<sup>f</sup> Flux density at  $\lambda = 1.1$  mm; from Sylvester et al. 1996.

<sup>g</sup> Herbig & Bell 1988.

<sup>h</sup> Osterloh & Beckwith 1995.

<sup>i</sup> Levraut 1988.

<sup>j</sup> See § 2, this work.

## 4. RESULTS AND ANALYSIS

## 4.1. Continuum Emission

Unresolved continuum emission was detected from all targets except the distant source LkH $\alpha$  259. Contour maps are presented in Figure 1, and measured flux densities are given in Table 2. Column (4) of Table 2 lists upper limits to radii, corresponding to half the FWHM of the minor axes of the synthesized beams. Assuming the source distances in Table 1, these limits range from 80 AU for CQ Tau to 1625 AU for MacC H12.

Within the errors, the continuum peak and the stellar position are spatially coincident for each Herbig Ae system. We therefore assume that all compact continuum sources in our sample are centered upon the target stars.

Our measured flux densities provide rough estimates of the masses of circumstellar material, assuming that emission at millimeter wavelengths is optically thin. Then,

$$M = \frac{F_\nu d^2}{\kappa_\nu B_\nu(T)}, \quad (1)$$

where  $d$  is the distance to the source, and  $\kappa$  is the mass opacity coefficient at frequency  $\nu$ . Assuming a gas-to-dust ratio of 100, by mass, and  $\kappa_{\lambda=0.25 \text{ mm}} = 0.1 \text{ cm}^2 \text{ g}^{-1}$ , we extrapolate to millimeter wavelengths using  $\kappa \propto \nu^\beta$  with  $\beta = 1$  (cf. Beckwith & Sargent 1991; Mannings & Emerson 1994). The same values of opacity and gas-to-dust ratio were used by BSCG, Osterloh & Beckwith (1995), and André & Montmerle (1994) to derive the masses of circumstellar material in T Tauri systems, permitting a direct comparison with the masses derived here (§ 5). Adopting for each source a characteristic temperature of 40 K (again, see Beckwith & Sargent 1991; Mannings & Emerson 1994), we obtain the mass estimates given in column (5) of Table 2, and they range from 0.009  $M_\odot$  (CQ Tau) to 0.234  $M_\odot$  (MacC H12). Note that, for  $\beta = 1$  and  $\lambda = 3 \text{ mm}$ ,  $\kappa = 0.0083 \text{ cm}^2 \text{ g}^{-1}$ , which is significantly higher than was suggested by the results of Pollack et al. (1994). The mass estimates presented here may, therefore, be conservatively low, probably by a factor of 3–4.

Using these measurements of mass and radius, we can compute values of  $A_V$  along the line of sight through a given

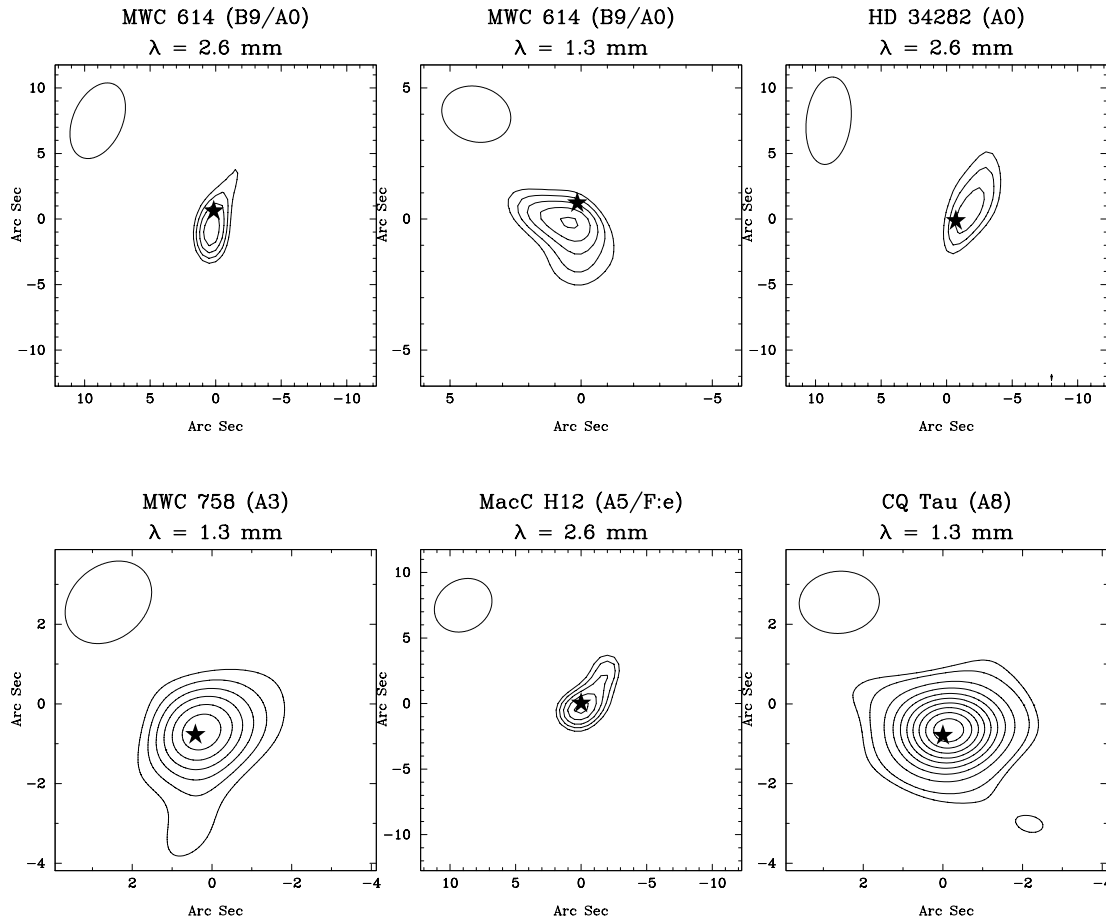


FIG. 1.—Contour plots of continuum emission. The centers of the maps correspond to the phase centers of the fields during the measurements with the array, which, in turn, are located at the stellar positions precessed from their equinox 1950.0 equatorial coordinates. The latter were taken from the *Hipparcos* Input Catalog for MWC 614 and HD 34282, and include proper motions to the epoch of the OVRO observations. Phase center coordinates for MWC 758 and CQ Tau were obtained from the SAO catalog. For MacC H12, we used the catalog of Herbig & Bell (1988). Offsets in units of arcseconds from the phase centers are indicated along the horizontal and vertical axes. Black asterisks represent stellar positions, corresponding simply to the phase center for MacC H12 and to newly available coordinates from the *Hipparcos* & *Tycho* Catalogues (ESA 1997) for MWC 614, HD 34282, MWC 758, and CQ Tau (including new values for proper motions). Ellipses in the upper left corners of the panels indicate position angles and FWHM of the synthesized beams. Contours on all maps begin at 3  $\sigma$ ; the 1  $\sigma$  rms noise and contour interval are, respectively, 1.2 mJy beam $^{-1}$  and 0.5  $\sigma$  for MWC 614 ( $\lambda = 2.6 \text{ mm}$ ), 5.3 mJy beam $^{-1}$  and 1  $\sigma$  for MWC 614 ( $\lambda = 1.3 \text{ mm}$ ), 3.5 mJy beam $^{-1}$  and 0.5  $\sigma$  for HD 34282, 4.7 mJy beam $^{-1}$  and 2  $\sigma$  for MWC 758, 1.5 mJy beam $^{-1}$  and 0.5  $\sigma$  for MacC H12, and 12.0 mJy beam $^{-1}$  and 2  $\sigma$  for CQ Tau. Flux densities are listed in Table 2.

TABLE 2  
CONTINUUM MEASUREMENTS AND DETERMINED QUANTITIES

Source (1)	$\lambda$ (mm) (2)	$F_\nu$ (mJy) (3)	$R_{\text{FWHM}}$ (AU) (4)	$M_{\text{dust + gas}}^a$ ( $M_\odot$ ) (5)	$A_V(s=0)^b$ (6)	$A_V(s=3/2)^c$ (7)
MWC 614 .....	2.6	$7.6 \pm 1.4$	$<450$	0.015	...	...
MWC 614 .....	1.3	$70.8 \pm 7.0$	$<230$	0.019	19	403
HD 34282 .....	2.6	$23.8 \pm 3.0$	$<270$	0.021	24	483
MWC 758 .....	1.3	$82.5 \pm 5.5$	$<185$	0.015	188	$>10^3$
MacC H12.....	2.6	$10.0 \pm 1.4$	$<1625$	0.234	17	698
CQ Tau .....	1.3	$143 \pm 8.4$	$<80$	0.009	253	$>10^3$
LkH $\alpha$ 259.....	2.6	$<6^d$	...	$<0.142$	...	...

<sup>a</sup> Assuming a gas-to-dust ratio of 100, by mass.

<sup>b</sup> As in Paper I, we adopt a power-law form for the radial density profile,  $\rho(r) \propto (r_0/r)^6$ . Here, we consider a uniform density spherical envelope of inner radius 1 AU.

<sup>c</sup> Freely falling spherical envelope of inner radius 1 AU.

<sup>d</sup> Upper limit of  $3\sigma$ .

continuum source to the central star, as in Paper I. In Table 2 we list  $A_V$  for uniform density and freely falling spherical envelopes. The extinctions range from around 20 to 250 mag for the physically unlikely case of uniform density envelopes, and from 400 to greater than 1000 mag for envelopes in free fall. Such values are far in excess of extinctions implied by the spectral types and observed colors, which are in the range 0.2 to 5.6 mag (§ 2 and Table 1). This suggests that most of the observed dust is distributed aspherically about the Herbig Ae stars, perhaps in the form of disks.

#### 4.2. Molecular Line Emission

Molecular line emission was detected in three of the six sources observed: MWC 758, MacC H12, and CQ Tau. Spatially integrated line spectra are plotted against velocity in Figure 2. Table 3 lists observed systemic velocities ( $v_0$ ), velocity ranges ( $\Delta v$ ) over which emission appears above the  $3\sigma$  level, and integrated intensities,  $\int S_\nu dv$ . Figure 3 displays contour maps of line emission integrated over the full velocity ranges, together with corresponding maps of the spatial distribution of intensity-weighted mean velocities across each of the gas structures. MWC 758 and MacC H12 are clearly spatially resolved, but are not circularly symmetric. CQ Tau is not spatially resolved. For all three sources, the separation of the stellar position and the centroid of the gas structure is much less than half the beam size. As for the dust regions, we assume that the molecular line emission arises in gas that is associated with and centered upon the stars.

Elliptical Gaussian brightness profiles were fitted to the maps of integrated intensity and then deconvolved from the Gaussian beams to obtain the radii at half-maximum intensity that are listed in column (6) of Table 3. The semimajor axes are 245 AU along P.A. =  $116^{+6}_-3$  deg and 4250 AU along P.A. =  $136^{+3}_-3$  deg for MWC 758 and MacC H12, respectively, assuming the distances listed in Table 1. For CQ Tau, we obtain an upper limit of 85 AU for the radius of the gas structure. The semiminor axis of the molecular emission from MWC 758 is 170 AU. From the aspect ratio, we obtain an inclination angle of  $i \approx \cos^{-1}(170/245) \approx 46^\circ$  (where  $0^\circ$  is face-on). MacC H12 has a semiminor axis of 2870 AU, suggesting an inclination angle  $i \approx 48^\circ$ .

The right-hand panels of Figure 3 show gray-scale maps of the spatial distribution of intensity-weighted mean

velocities across each of the three gas structures—i.e., first-moment maps with respect to gas velocity. Such maps are crude in the sense that at each point we characterize the full range of gas velocities along the line of sight by just one value, but they provide a useful probe for ordered bulk-gas motions if the major axis can be identified unambiguously (cf. Koerner & Sargent 1995; Koerner 1997). Our first-moment maps indicate ordered velocity gradients in all three cases. For both MWC 758 and CQ Tau, blueshifted emission is confined to the east of the star, while redshifted emission is found only to the west. The above-mentioned Gaussian fit to the zeroth-moment map of CQ Tau is dominated by the bright and unresolved core of the emission profile, but, in the first-moment map, the emission is marginally resolved along the major axis. The upper limit of 85 AU for the radius is probably close to the actual value. The spatial compactness, the narrow line widths (see also below), and the ordered velocity gradients along the major axes strongly support the hypothesis that the material around MWC 758 and CQ Tau is rotating in Keplerian orbits. By contrast, MacC H12 has an irregular shape, and the gradient is orthogonal to the apparent major axis. This source is discussed further in § 5.

The CO line profiles for MWC 758 and CQ Tau are a particularly useful diagnostic. There is no evidence of the extended velocity wings characteristic of outflow motions (cf. Bachiller 1996). Although the two remaining kinematic options, infall and rotation, should generate double-peaked lines (e.g., Beckwith & Sargent 1993b), neither MWC 758 nor CQ Tau displays this feature, presumably because of insufficient velocity resolution. However, the width of the line for MWC 758 can help discriminate between infall and rotation. Using the stellar mass given in Table 1 and the disk radius and inclination angle from Table 3, the angle-adjusted Keplerian velocity,  $(GM_*/R_D)^{0.5}$ , is  $v_{\text{Kep}} = 1.9 \text{ km s}^{-1}$ . This is just a little higher than half the line width, or  $1.3 \text{ km s}^{-1}$ , for the spectrum shown in Figure 2, and it is substantially less than the theoretical infall velocity  $v_{\text{inf}} = \sqrt{2}v_{\text{Kep}} = 2.7 \text{ km s}^{-1}$ . Keeping in mind that these calculations are rough and that they involve a mix of quantities derived from a spectrum, a map, and the H-R diagram (§ 5), the fact that  $v_{\text{obs}} < v_{\text{Kep}} < v_{\text{inf}}$  argues for gas moving in Keplerian orbits around MWC 758. These arguments cannot, however, be applied to CQ Tau, where the emission is spatially unresolved and the inclination angle is unknown.

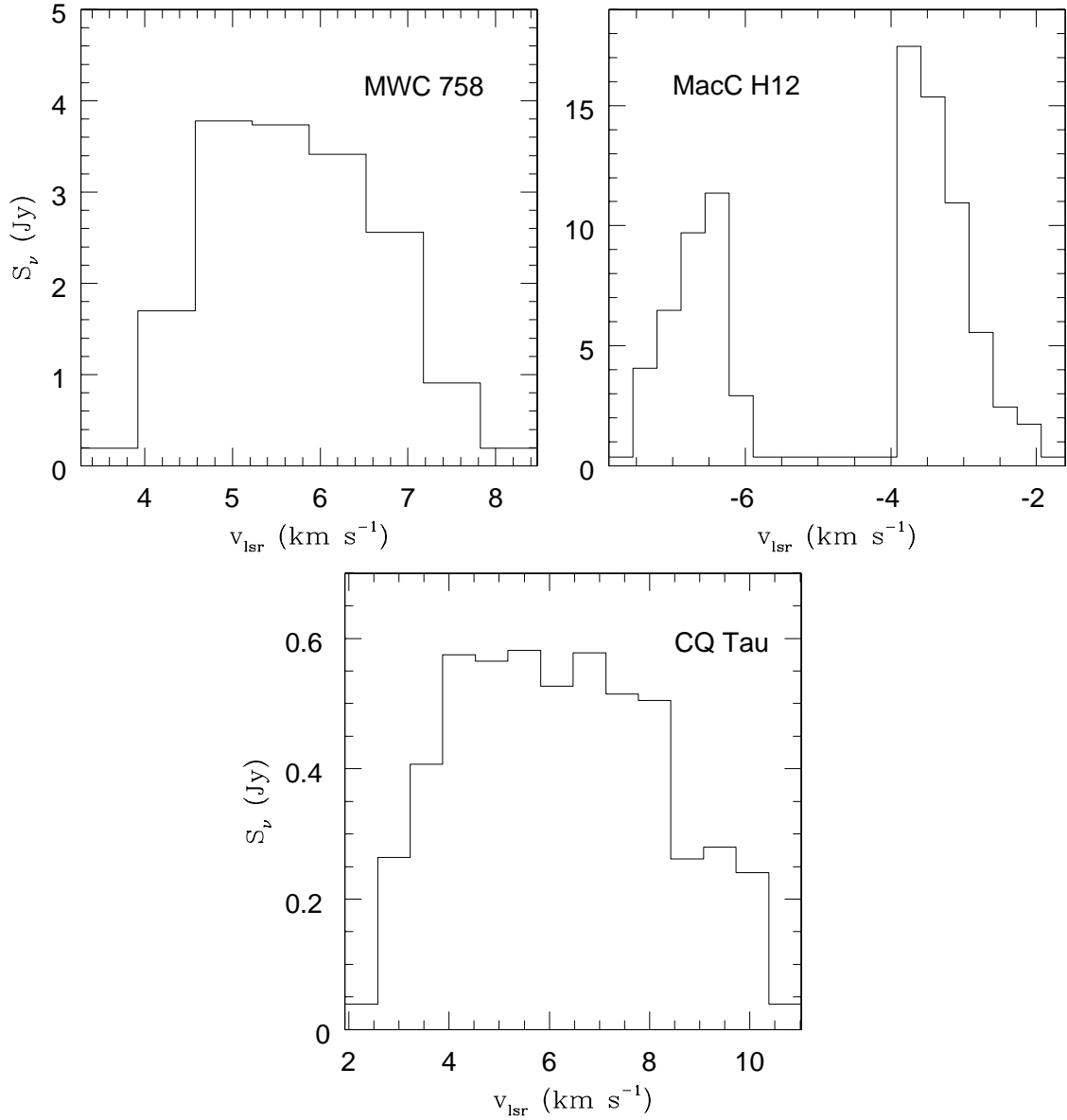


FIG. 2.—Spatially integrated spectra. MWC 758 and CQ Tau were observed in CO (2 → 1), while MacC H12 was mapped in CO (1 → 0). The flux density scale, in Jy, ranges by about 1 order of magnitude to allow easy comparison of the line shapes for the three Herbig Ae systems.

TABLE 3  
MOLECULAR LINE MEASUREMENTS AND DETERMINED QUANTITIES

Source (1)	Line (2)	$v_0$ (LSR) (km s <sup>-1</sup> ) (3)	$\Delta v$ (LSR) <sup>a</sup> (km s <sup>-1</sup> ) (4)	$\int S_\nu dv$ (Jy km s <sup>-1</sup> ) (5)	$R_{\text{FWHM}}$ (AU) (6)	P.A. (deg) (7)	$i$ (deg) (8)	$M_{\text{H}_2}$ ( $M_\odot$ ) (9)
MWC 614 .....	CO (1 → 0)	...	...	<0.279 <sup>b</sup>	...	...	...	...
HD 34282 .....	CO (1 → 0)	...	...	<0.486 <sup>b</sup>	...	...	...	...
MWC 758 .....	CO (2 → 1)	+5.9	+4.2 to +7.5	10.8	245 × 170	116 $^{+6}_{-5}$	46	3.97 × 10 <sup>-5</sup>
MacC H12 .....	CO (1 → 0)	-4.7	-2.1 to -7.3	49.5	4250 × 2870	136 $^{+3}_{-3}$	48	3.64 × 10 <sup>-2</sup>
CQ Tau .....	CO (2 → 1)	+5.9	+2.9 to +10.1	32.3	<85	...	...	2.62 × 10 <sup>-5</sup>
LkH $\alpha$ 259 .....	CO (1 → 0)	...	...	<0.256 <sup>b</sup>	...	...	...	...

<sup>a</sup> Full width of line for which emission is above the 3  $\sigma$  level.

<sup>b</sup> Upper limit, per beam, at 3  $\sigma$  across a channel of width 1.3 km s<sup>-1</sup>.

Total masses of circumstellar gas can be determined from the observed velocity-integrated emission,  $\int S_\nu dv$ , and the following conversions (cf. Scoville et al. 1986) for CO (1  $\rightarrow$  0) and CO (2  $\rightarrow$  1), respectively:

$$M_{\text{H}_2}(M_\odot) = 2.19 \times 10^{-5} \frac{(T_x + 0.93)}{e^{-5.59/T_x}} \frac{\tau_{\text{CO}}}{(1 - e^{-\tau})} d_{\text{kpc}}^2 \int S_\nu dv \quad (2)$$

and

$$M_{\text{H}_2}(M_\odot) = 1.42 \times 10^{-10} \frac{(T_x + 0.93)}{e^{-16.76/T_x}} \frac{\tau_{\text{CO}}}{(1 - e^{-\tau})} \times \frac{d_{\text{kpc}}^2}{X_{\text{CO}}} \int S_\nu dv, \quad (3)$$

where  $S_\nu$  is in units of Jy,  $v$  is in  $\text{km s}^{-1}$ ,  $T_x$  is the excitation temperature,  $\tau$  is optical depth in the given line, and  $X$  is the

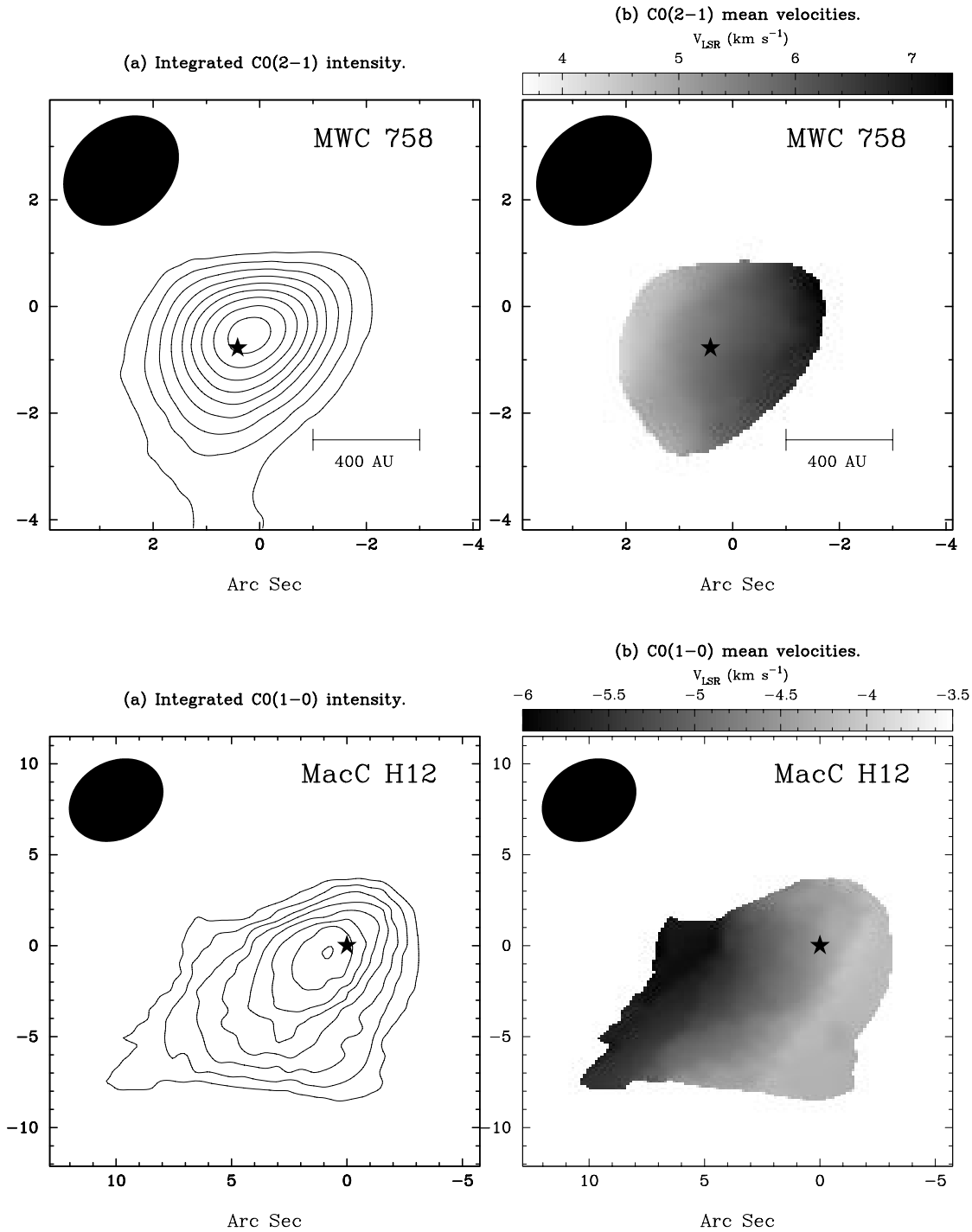


FIG. 3.—Molecular line emission maps. The panels show contours of velocity-integrated intensities (left) and gray scales of intensity-weighted mean velocities (right). Offsets in arcseconds from the phase centers are indicated along the horizontal and vertical axes. Star symbols represent stellar positions (see caption to Fig. 1). The FWHM and orientations of the synthesized beams are indicated in the upper left corner of each map. Contours begin at a level of  $3\sigma$ ; intensities are listed in Table 3.

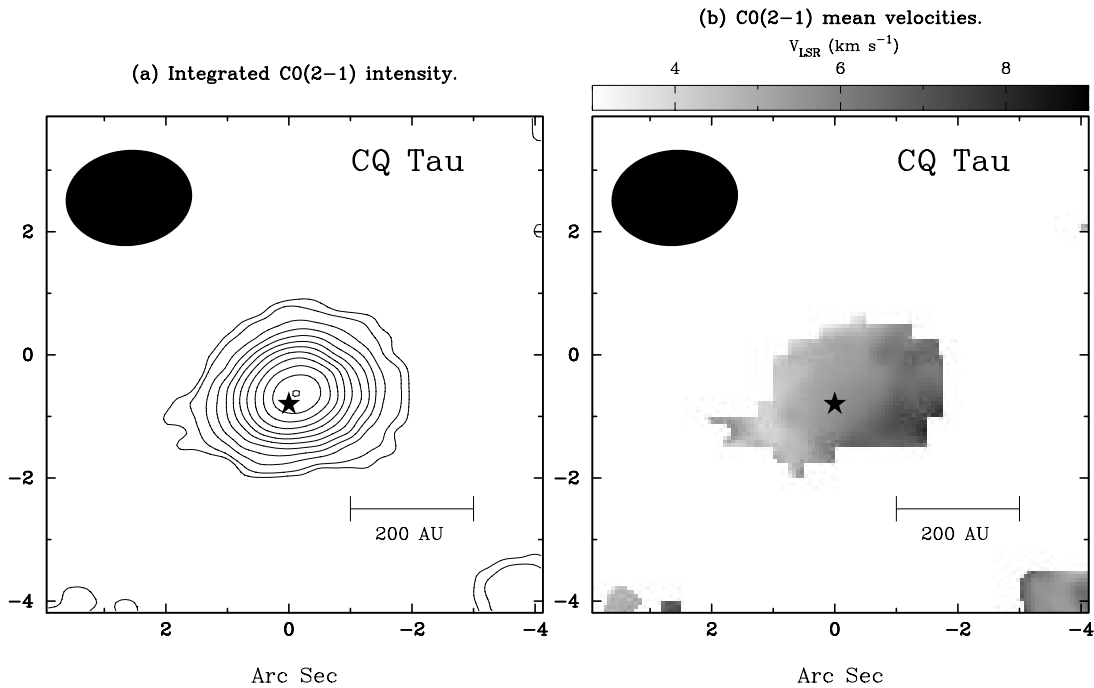


FIG. 3.—Continued

fractional abundance relative to molecular hydrogen. In the optically thin limit, the mass is straightforwardly calculable; here only lower limits to masses of molecular hydrogen can be computed. These are presented in column (9) of Table 3, where we have assumed for all four sources an excitation temperature of 40 K. The fractional abundance of CO is taken to be  $10^{-4}$ .

The computed gas masses in Table 3 disagree, sometimes by orders of magnitude, with those determined using our continuum flux densities (see Table 2). The ratios of total masses derived from continuum and spectral line measurements are 378 for MWC 758, 6 for MacC H12, and 344 for CQ Tau. Similar discrepancies were found for Herbig Ae sources (Paper I) and for T Tauri systems (Dutrey, Guillo-teau, & Simon 1994; Koerner & Sargent 1995; Dutrey et al. 1996). Suggested causes are CO depletion onto grains at low temperatures or contributions to observed line emission from optically thick regions of molecular gas (Dutrey et al. 1996; Sargent 1996 and references therein). Mass determinations based on observations using optically thin line emission from other CO isotopomers or other molecules are probably necessary to clarify this issue. In the meantime we assume that the continuum fluxes, which are very likely optically thin, provide more reliable estimates of the masses of circumstellar material despite uncertainties in the value of  $\kappa_v$ .

## 5. DISCUSSION

The observations described here identify compact sources of millimeter-wave emission centered upon most of the Herbig Ae stars in our sample. As in Paper I, we see directly that continuum and, in several cases, molecular line emission arises from material located typically within a few hundred AU of each target. Estimated masses of circumstellar gas and dust, based on the continuum measurements, would lead to  $V$ -band extinctions of up to  $10^3$  mag and more if the circumstellar material is distributed spherically. Observed values of  $A_V$  are in the range 0.2–5.5 (Table 1), suggesting relatively flattened and inclined sources of emission. Elongated morphology is in fact seen in the MWC 758 image; both the CO line width and a velocity gradient along the major axis also argue for the presence of a rotating disk. Evidence for Keplerian gas motions is less compelling for CQ Tau, but the compactness of the source in continuum and CO line emission ( $r \lesssim 100$  AU) is consistent with expectations for a rotating disk, such as those seen in other Herbig Ae and T Tauri systems.

The properties of the circumstellar material in MacC H12 are very different. Our CO map reveals an aspherical source of size  $4250 \times 2870$  AU, an order of magnitude greater than usual for Herbig Ae and T Tauri systems, while the continuum flux implies a mass about 10 times higher (cf. Table 4).

TABLE 4  
COMPARISON OF Ae DISK PROPERTIES WITH TTs DISKS

Systems	Average Mass (Gas + Dust) ( $M_\odot$ )	Mass Range ( $M_\odot$ )	Radii of Dust Components (AU)	Radii of Molecular Gas Components (AU)
Ae <sup>a</sup> .....	0.020	0.009–0.034	$\lesssim 300$	85–450
T Tauri.....	0.010 <sup>b</sup>	0.001–0.038 <sup>b</sup>	$\leq 180^c$	110–350 <sup>c</sup>

<sup>a</sup> Sources are from Paper I and the present work. MacC H12 is excluded.

<sup>b</sup> Using 1.3 mm flux densities from Beckwith et al. 1990; see Paper I.

<sup>c</sup> From results of Koerner & Sargent 1995.

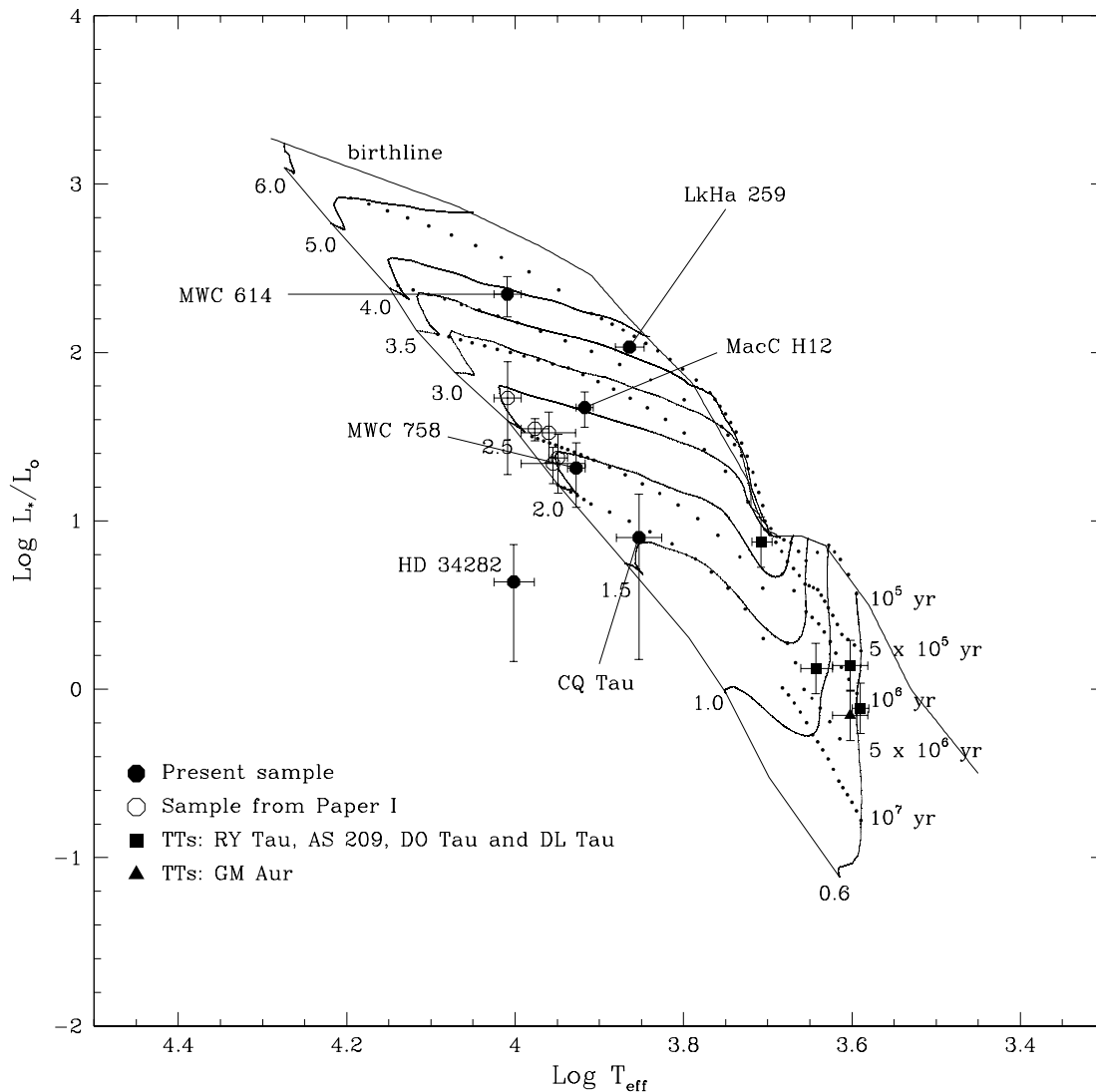


FIG. 4.—H-R diagram, with stellar temperatures and luminosities for the present sample, taken from Table 1; see also § 5. Mass tracks and isochrones are from F. Palla (1999, private communication; see Palla & Stahler 1993). Zero-age main sequence (ZAMS) stellar masses are indicated along the main sequence in units of  $M_{\odot}$ .

The orientation of the velocity gradient along the minor axis in the first-moment map of Figure 3 suggests that MacC H12 is a very young star, perhaps still embedded within an infalling envelope (cf. Hayashi, Ohashi, & Miyama 1993). In this case, we anticipate a class I SED (Lada 1987), rising sharply at far-IR wavelengths. However, the IR–millimeter SED of MacC H12 (Pezzuto et al. 1997) strongly resembles the class II SEDs that are typical of T Tauri star/disk systems, where emission falls off with increasing wavelength. Indeed, it is very similar to the IR–millimeter SEDs of the star/disk Ae systems AB Aur and HD 163296 (Mannings 1994; Paper I). Additionally, if it is embedded (and therefore, presumably, young), we would expect MacC H12 to be on or close to the Stahler birth line on the Hertzsprung-Russell diagram. We show the locations<sup>1</sup> of all our target stars on the H-R plane in Figure 4. MacC H12 appears far below the birth line, with an age of about 3 Myr. It is unlikely that a star of this age would be accompanied by the extended structure revealed in Figure 3. Possible explanations include source confusion (the millimeter-wave source is not associated with the cataloged

Ae star MacC H12) or incorrect spectral type and/or  $A_V$ , each of which would invalidate the position plotted on the H-R diagram. Observations with greater sensitivity and better resolution clearly are required in order to search for multiple sources and to examine gas kinematics in more detail.

All objects in our present sample are plotted as filled circles in Figure 4. Sources from Paper I are represented by open circles. As already noted by van den Ancker, de

<sup>1</sup> Spectral types were converted to photospheric effective temperatures using the results of Cohen & Kuhn (1979). Uncertainties in  $T_{\text{eff}}$  were estimated from the range of spectral types claimed in the literature for each Ae star. Stellar radii and luminosities were derived by fitting dereddened optical magnitudes. Uncertainties in luminosities were estimated using both the range of spectral types and the known optical variability (Thé et al. 1994). Theoretical pre-MS mass tracks and isochrones plotted on the H-R diagram in Fig. 4 are from digital files kindly made available by F. Palla (see also Palla & Stahler 1993). In Paper I we used mass tracks by D’Antona & Mazzitelli (1994), which include stars up to masses of  $2.5 M_{\odot}$ . The mass tracks used here extend to masses of  $6 M_{\odot}$  and are needed in order to obtain masses for our full sample of stars. Our estimates of stellar radii, luminosities, masses, and ages are given in Table 1.

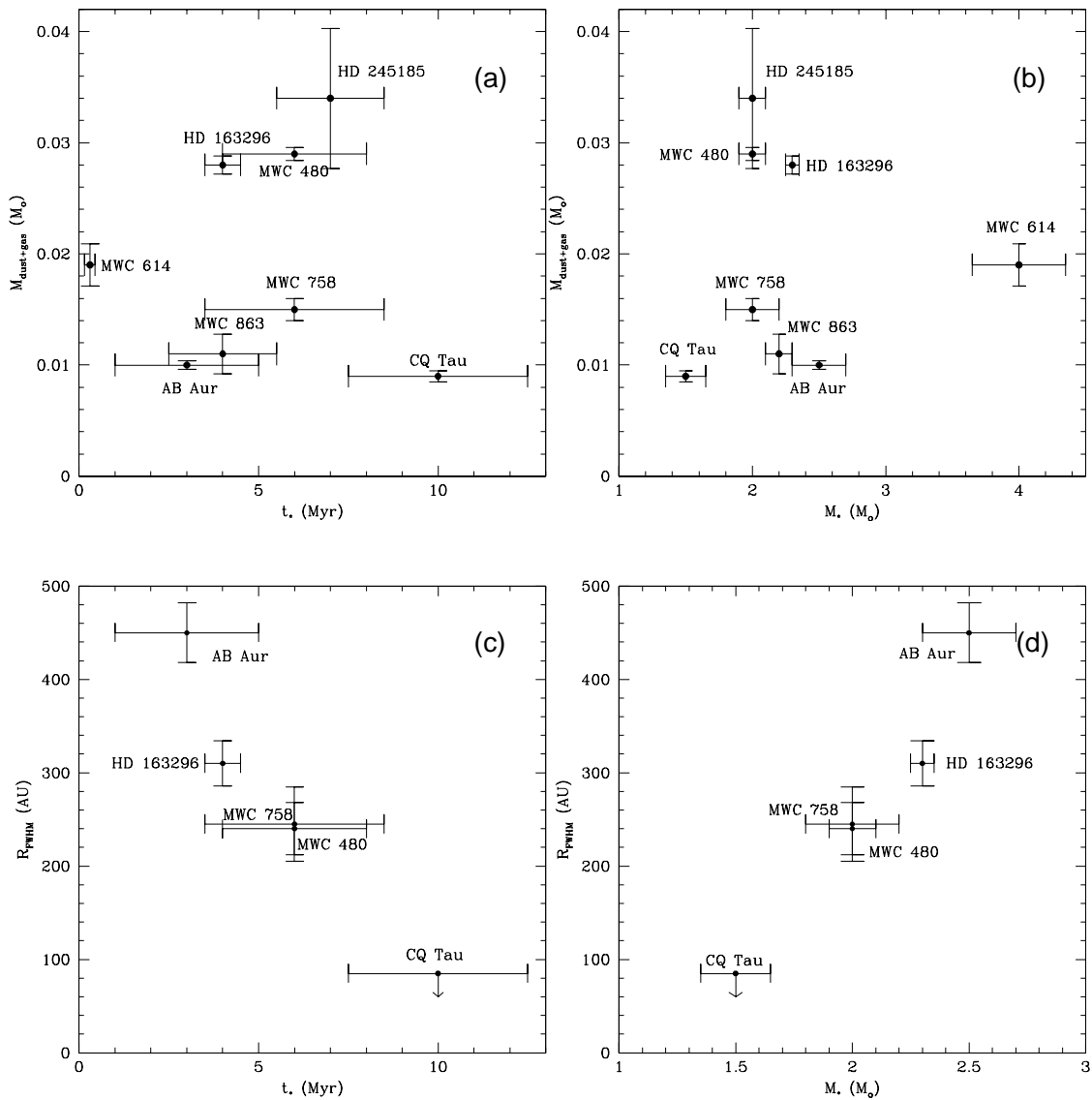


FIG. 5.—Disk masses and radii plotted against stellar ages and stellar masses. See discussion in § 5

Winter, & Tjin A Djie (1998), HD 34282 appears well below the main sequence. This is probably due to a misclassification of spectral type or to an error in the distance determination. Stellar masses and ages inferred from Figure 4 range from  $1.5 M_{\odot}$  (CQ Tau) to  $4 M_{\odot}$  (MWC 614) and from 0.3 Myr (LkH $\alpha$  259 and MWC 614) to 10 Myr (CQ Tau), respectively.

Within the set of sources discussed here and in Paper I, can we discern any trends of disk properties with age and stellar mass? Figure 5 shows plots of circumstellar mass and source radius as functions of stellar age and mass.<sup>2</sup> Because of the uncertainties, we exclude MacC H12. No correlations between circumstellar mass and stellar age, or between circumstellar mass and stellar mass, are evident in Figures 5a

and 5b. The same conclusion was drawn for TTs disks by BSCG for the same range of ages. The mass range for Ae disks in the present work is within the mass range of Paper I, and this range is indistinguishable from the masses of TTs disks (Table 4). Disk masses may therefore be independent of stellar mass from  $M_{*} \approx 0.5$  to  $4 M_{\odot}$ . Disk radii extend across a range similar to that measured for TTs disks (Table 4). In Figure 5c, disk radius appears to decrease with age, but the trend relies heavily upon the first and last data points (AB Aur and CQ Tau, respectively). The radius of CQ Tau's disk is by far the smallest of any of the Ae systems imaged to date and is also smaller than any of the TTs disks (cf. Koerner & Sargent 1995). While CQ Tau is the oldest Ae star in our sample, we are reluctant to attribute the small size to disk evolution, given the limited sample here. The disk may simply be at the low end of the range of masses and radii exhibited by Ae disks. Likewise, the sample size prevents any firm conclusion from being drawn from Figure 5d, where there appears to be a correlation between Ae disk radii and stellar masses.

Note, when interpreting Figure 5, that there are two caveats. First, the disk masses are derived from spatially

<sup>2</sup> In Paper I we used the mass tracks and isochrones of D'Antona & Mazzitelli (1994). For consistency within the combined sample, we use the masses and ages of the Paper I sample implied by the tracks of Palla & Stahler (1993), plotted in Fig. 4. They are  $2.5 M_{\odot}$  and 3 Myr (AB Aur),  $2.3 M_{\odot}$  and 4 Myr (HD 163296),  $2.2 M_{\odot}$  and 4 Myr (MWC 863),  $2.0 M_{\odot}$  and 7 Myr (HD 245185), and  $2.0 M_{\odot}$  and 6 Myr (MWC 480). These values are in fact very similar to those deduced in Paper I.

unresolved continuum measurements, while the radii are from the CO images. However, the two derived quantities essentially characterize the same source: since the density profiles rise sharply with decreasing radius, most of a disk's mass is contained within the unresolved region measured by continuum observations. At the same time, dust and gas are spatially coincident out to the CO radius, although the emission of the dust falls off more rapidly. Second, from the perspective of disk properties, stellar age and stellar mass are not necessarily independent parameters. Given a sufficiently large sample of stars with a good spread in both age and mass, it should be possible to explore the variation of disk mass and disk radius with respect to, separately, age and stellar mass. We have therefore used our small sample here to make only a first step in searching for trends.

## 6. SUMMARY AND CONCLUSIONS

As a follow-up to our study of seven Herbig Ae systems (Paper I), we have imaged four additional Ae sources at high spatial resolution and mapped two of the original seven sources, MWC 758 and CQ Tau, in the 1.3 mm band to achieve higher resolution. Thermal continuum emission from dust was detected from all except one source, LkH $\alpha$  259, which is very distant. Molecular line emission was measured toward MacC H12, as well as from MWC 758 and CQ Tau. All detected dust and gas regions are centered on the target stars. The dust regions are not resolved, and we place upper limits to radii ranging from 80 AU for the nearest source, CQ Tau, to 1625 AU for MacC H12. Continuum fluxes imply masses of dust and gas in the range 0.009–0.021  $M_{\odot}$  for, in order of increasing mass, CQ Tau, MWC 758, MWC 614, and HD 34282.

Molecular line emission from MWC 758 is spatially resolved and elongated, with a semimajor axis of 245 AU. The aspect ratio yields an inclination angle of 46°. A velocity gradient along the major axis is observed, which is consistent with the presence of a rotating disk of circumstellar material. The CO map for CQ Tau is dominated by a bright and unresolved central core of emission with radius  $\leq 85$  AU. There is weak evidence for a velocity gradient. We suggest that CQ Tau, like MWC 758, is surrounded by a Keplerian disk and that the circumstellar environments of MWC 614 and HD 34282 include substantial disk components. Indeed, visual extinctions computed for spherical distributions of material with the above radii and masses

are much higher than the actual extinctions observed toward each of the stars in our sample. Note also that single-dish CO (3  $\rightarrow$  2) measurements of HD 34282 (Greaves, Mannings, & Holland 2000), display the narrow and double-peaked profile characteristic of gas that is rotating or infalling in a plane. Higher resolution observations of HD 34282 in CO (2  $\rightarrow$  1) and 1.3 mm continuum emission should clarify this situation. The gas and dust region nominally associated with the distant star MacC H12 is an order of magnitude greater in size and mass than the disks encircling MWC 758 and CQ Tau, and we propose that the central star is relatively young and still embedded within an envelope. The star itself may not be the cataloged Ae star MacC H12.

Combining the new results with those of Paper I provides a sample of some 11 Herbig Ae systems. Excluding MacC H12, they range in age from 0.3 to 10 Myr, with stellar masses from 1.5 to 4  $M_{\odot}$ . Although the sample is small, and biased by the selection criteria, it seems that disk masses are uncorrelated with both stellar age and with stellar mass, similar to TTs aged 10 Myr and less. The Herbig Ae disk masses are indistinguishable from TTs disk masses, so that disk masses appear to be independent of the masses of the central stars across the range  $0.5 \lesssim M_{*}/M_{\odot} \lesssim 4$ . For the subset of five sources with spatially resolved gas regions, AB Aur, HD 163296, MWC 480, MWC 758, and CQ Tau, there is some indication of a decrease of disk radius with age and an increase of radius with stellar mass. However, these trends remain to be confirmed with a larger and better-populated sample of stellar ages and masses.

The Owens Valley millimeter-wave array is supported by NSF grant AST 96-13717. Research at Owens Valley on young star and disk systems is also supported by the Norris Planetary Origins Project, for which we are very grateful. We are also grateful to NASA's Origins of Solar Systems program, which provides funding through grant NAGW-4559. An anonymous referee is thanked for useful suggestions. We thank Francesco Palla for kindly providing pre-MS mass tracks and isochrones. Jane Greaves and Roger Sylvester are thanked for useful discussion and comments. This research has made use of NASA's Astrophysics Data System Abstract Service, together with the SIMBAD database operated at CDS, Strasbourg, France.

## REFERENCES

- Adams, F. C., Lada, C. J., & Shu, F. H. 1987, *ApJ*, 312, 788  
 ———, 1988, *ApJ*, 326, 865  
 André, P., & Montmerle, T. 1994, *ApJ*, 420, 837  
 Bachiller, R. 1996, *ARA&A*, 34, 111  
 Backman, D. E., & Paresce, F. 1993, in *Protostars and Planets III*, ed. E. H. Levy & J. I. Lunine (Tucson: Univ. Arizona Press), 1253  
 Beckwith, S. V. W., & Sargent, A. I. 1991, *ApJ*, 381, 250  
 ———, 1993a, in *Protostars and Planets III*, ed. E. H. Levy & J. I. Lunine (Tucson: University of Arizona Press), 521  
 ———, 1993b, *ApJ*, 402, 280  
 Beckwith, S. V. W., Sargent, A. I., Chini, R. S., & Güsten, R. 1990, *AJ*, 99, 924 (BSCG)  
 Berrilli, F., Corciulo, G., Ingrassio, G., Lorenzetti, D., Nisini, B., & Strafella, F. 1992, *ApJ*, 398, 254  
 Calvet, N., Hartmann, L., Kenyon, S. J., & Whitney, B. 1994, in *ASP Conf. Ser. 62, The Nature and Evolutionary Status of Herbig Ae/Be Stars*, ed. P. S. Thé, M. R. Pérez, & E. P. J. van den Heuvel (San Francisco: ASP), 207  
 Cohen, M., & Kuhl, L. V. 1979, *ApJS*, 41, 743  
 D'Antona, F., & Mazzitelli, I. 1994, *ApJS*, 90, 467  
 Di Francesco, J., Evans, N. J., Harvey, P. M., Mundy, L. G., & Butner, H. M. 1994, *ApJ*, 432, 710  
 Dutrey, A., Guilloteau, S., Duvert, G., Prato, G., Simon, M., Schuster, K., & Ménard, F. 1996, *A&A*, 309, 493  
 Dutrey, A., Guilloteau, S., Prato, L., Simon, M., Duvert, G., Schuster, K., & Ménard, F. 1998, *A&A*, 338, L63  
 Dutrey, A., Guilloteau, S., & Simon, M. 1994, *A&A*, 286, 149  
 ESA. 1997, *The Hipparcos and Tycho Catalogues* (ESA SP-1200; Noordwijk: ESA)  
 Greaves, J. S., Mannings, V., & Holland, W. S. 2000, *Icarus*, in press  
 Hayashi, M., Ohashi, N., & Miyama, S. M. 1993, *ApJ*, 418, L71  
 Herbig, G. H. 1960, *ApJS*, 4, 337  
 ———, 1994, in *ASP Conf. Ser. 62, The Nature and Evolutionary Status of Herbig Ae/Be Stars*, ed. P. S. Thé, M. R. Pérez, & E. P. J. van den Heuvel (San Francisco: ASP), 3  
 Herbig, G. H., & Bell, K. R. 1988, *Lick Obs. Bull.*, No. 1111  
 Hillenbrand, L. A., Strom, S. E., Vrba, F. J., & Keene, J. 1992, *ApJ*, 397, 613  
 Koerner, D. W. 1997, in *IAU Symp. 170, CO: 25 Years of Millimeter-Wave Spectroscopy*, ed. W. B. Latter, J. E. Radford Simon, P. R. Jewell, J. G. Mangum, & J. Bally (Dordrecht: Kluwer), 162  
 Koerner, D. W., & Sargent, A. I. 1995, *AJ*, 109, 2138  
 Lada, C. J. 1987, in *IAU Symp. 115, Star Forming Regions*, ed. M. Peimbert & J. Jugaku (Dordrecht: Kluwer), 1

- Lagrange, A.-M., Backman, D., & Artymowicz, P. 2000, in *Protostars and Planets IV*, ed. V. Mannings, A. P. Boss, & S. S. Russell (Tucson: Univ. Arizona Press), in press
- Levreault, R. M. 1988, *ApJS*, 67, 283
- Mannings, V. 1994, *MNRAS*, 271, 587
- Mannings, V., & Emerson, J. P. 1994, *MNRAS*, 267, 361
- Mannings, V., Koerner, D. W., & Sargent, A. I. 1997, *Nature*, 388, 555
- Mannings, V., & Sargent, A. I. 1997, *ApJ*, 490, 792 (Paper I)
- Miroshnichenko, A., Ivezić, Z., & Elitzur, M. 1997, *ApJ*, 475, L41
- Natta, A., Grinin, V. P., & Mannings, V. 2000, in *Protostars and Planets IV*, ed. V. Mannings, A. P. Boss, & S. S. Russell (Tucson: Univ. Arizona Press), in press
- Natta, A., Grinin, V. P., Mannings, V., & Ungerechts, H. 1997, *ApJ*, 491, 885
- Natta, A., Palla, F., Butner, H. M., Evans, N. J., & Harvey, P. M. 1992, *ApJ*, 391, 805
- . 1993, *ApJ*, 406, 674
- Osterloh, M., & Beckwith, S. V. W. 1995, *ApJ*, 439, 288
- Palla, F., & Stahler, S. W. 1993, *ApJ*, 418, 414
- Pérez, M. R., & Grady, C. A. 1997, *Space Sci. Rev.*, 82, 407
- Pezzuto, S., Strafella, F., & Lorenzetti, D. 1997, *ApJ*, 485, 290
- Pollack, J. B., Hollenbach, D., Beckwith, S. V. W., Simonelli, D. P., & Fong, W. 1994, *ApJ*, 421, 615
- Sargent, A. I. 1996, in *Disks and Outflows around Young Stars*, ed. S. V. W. Beckwith, J. Staude, A. Quetz, & A. Natta (Berlin: Springer), 1
- Schmidt-Kaler, T. 1982, in *Landolt-Börnstein, Numerical Data and Functional Relationships in Science and Technology, Group VI, Astronomy, Astrophysics and Space Research, Vol. 2b*, ed. K. Schaifers & H. H. Voigt (Berlin: Springer), 15
- Scoville, N. Z., Carlstrom, J. E., Chandler, C. J., Phillips, J. A., Scott, S. L., Tilanus, R. P. J., & Wang, Z. 1993, *PASP*, 105, 1482
- Scoville, N. Z., Sargent, A. I., Sanders, D. B., Claussen, M. J., Masson, C. R., Lo, K. Y., & Phillips, T. G. 1986, *ApJ*, 303, 416
- Strom, S. E., Edwards, S., & Skrutskie, M. F. 1993, in *Protostars and Planets III*, eds. E. H. Levy & J. I. Lunine (Tucson: Univ. Arizona Press), 837
- Sylvester, R. J., Skinner, C. J., Barlow, M. J., & Mannings, V. 1996, *MNRAS*, 279, 915
- Thé, P. S., de Winter, D., & Pérez, M. R. 1994, *A&AS*, 104, 315
- van den Ancker, M. E., de Winter, D., & Tjin A Djie, H. R. E. 1998, *A&A*, 330, 145
- Waters, L. B. F. M., & Waelkens, C. 1998, *ARA&A*, 36, 233